Iron-Brønsted-acid-catalysed asymmetric hydrogenation: Mechanism and selectivity-determining interactions

Kathrin H. Hopmann*[a]

Abstract

Hydrogenation catalysts involving abundant base metals such as cobalt or iron are promising alternatives to precious metal systems. Despite rapid progress in this field, base metal catalysts do not yet achieve the activity and selectivity levels of their precious metal counterparts. Rational improvement of base metal complexes is facilitated by detailed knowledge about their mechanisms and selectivity-determining factors. The mechanism for asymmetric imine hydrogenation with Knölker's iron complex in presence of a chiral phosphoric acid is here investigated computationally at the DFT-D level of theory, with models of up to 160 atoms. The resting state of the system is found to be an adduct between the iron complex and the deprotonated acid. Rate-limiting H_2 splitting is followed by a step-wise hydrogenation mechanism, where the phosphoric acid acts as the proton donor. C-H…O interactions between the phosphoric acid and the substrate are involved in the stereocontrol at the final hydride transfer step. Computed enantiomeric ratios show excellent agreement with experiment, indicating that DFT-D is able to correctly capture the selectivity-determining interactions of this system.

Introduction

Homogenous asymmetric hydrogenation involves reduction of pro-chiral imines, alkenes, and ketones to the corresponding chiral amines, alkanes, and alcohols. Reactions of this type are essential in the synthesis of many different compounds such as fine chemicals, fragrance and flavour molecules, agrochemicals, and pharmaceuticals.[1,2] A well-known example is the enantioselective iridium-catalysed hydrogenation leading to the synthesis of the herbicide (*S*)-metolachlor, representing one of the largest scale hydrogenations employed industrially.[2] A similarly well-known example is the first industrially implemented protocol for L-DOPA synthesis, which involved a rhodium-diphosphine-catalysed hydrogenation step. [2]

The majority of catalysts employed in asymmetric hydrogenation reactions are based on precious metals such as rhodium,[1] iridium,[3] and ruthenium.[4] The cost of precious metals has fuelled academic and industrial research into alternative hydrogenation catalysts involving abundant base metals such as cobalt and iron.[5] Base metals are considered to be less toxic and of less environmental concern, and are hence more in line with a green chemistry approach.

Examples of recent base metal hydrogenation catalysts are the bis[2-(dicyclohexyl-phosphine)ethyl]amine cobalt(II) complexes for hydrogenation of imines, ketones, and alkenes reported by Hanson and co-workers. [6,7] Asymmetric cobalt catalysts have been reported by Chirik and co-workers.[8,9] Chirik's chiral bis-imino-pyridine cobalt complexes gave promising enantiomeric excesses in the hydrogenation of styrene-derived terminal alkenes.[8] Milstein has reported pincer-based iron hydrogenation catalysts for symmetric reduction of ketones.[10,11] Morris and co-workers have applied chiral iron-based hydrogenation catalysts with tridentate [Fe(P-N-P)] and tetradentate [Fe(P−N−N−P) ligands in the asymmetric hydrogenation of ketones and imines.[12,13] Casey and Guan reported symmetric hydrogenation of aldehydes, ketones, and imines with Knölker's iron complex, which possesses a cyclopentadienone ligand.[14,15] Berkessel has reported a related iron cyclopentadienone complex with a chiral phosphoramidite ligand, which was applied in the asymmetric reduction of ketones. [16] This type of iron cyclopentadienone catalysts can be seen as cheap and relatively easily accessible derivatives of the original ruthenium-based Shvo's catalyst (for a recent review see [17]).

An interesting modular approach to asymmetric hydrogenation involves combination of an achiral metal catalyst with a chiral additive such as a chiral Brønsted acid.[18] Formation of a supramolecular complex, held together through non-covalent interactions, provides altered activity and/or reactivity of the combined system, relative to the individual fragments.[19] For example, Beller and co-workers have combined Knölker's complex with chiral BINOL-derived phosphoric acids in the asymmetric hydrogenation of acyclic and cyclic imines (Figure 1). [20,21,22] For quinoxalines, enantiomeric excesses (ee's) of up to 90% were obtained.[22]

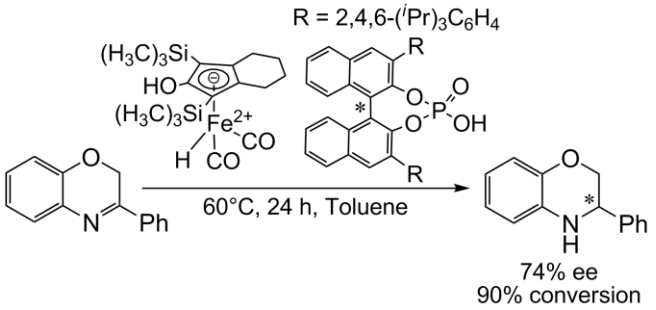

Figure 1. Cooperative iron–Brønsted acid–mediated hydrogenation of 3-phenyl-2H-benzo[b][1,4]oxazine (from [22]).

[a] Dr. Kathrin H. Hopmann
Department of Chemistry and Centre for Computational and Theoretical Chemistry (CTCC)
University of Tromsø, N-9037 Tromsø Norway
E-mail: kathrin.hopmann@uit.no

Supporting information for this article is given via a link at the end of the document.

The reported base metal hydrogenation catalysts have been shown to have promising properties, however, many of these complexes do not yet achieve the activity, substrate scope, and selectivity level of their precious metal counterparts. For example, for iron-Brønsted-acid-catalysed hydrogenation of 2H-1,4-benoxazines, Beller and co-workers have reported ee's of up to 74 % (90% conversion, 60°, Figure 1).[22] For the same substrate class, iridium-P-OP-catalysed hydrogenations give far superior results, e.g. achieving an ee of 99% for 3-phenyl-2H-benzo[b][1,4]oxazine (98% conversion, room temperature).[23]

Improvement of base metal catalysts through rational design is facilitated if detailed knowledge about mechanisms and selectivity-determining factors is available. Quantum mechanical (QM) calculations provide an excellent tool to obtain such insights (for reviews on the use of QM methods to study asymmetric reactions see e.g. [24]; for some of the seminal papers in this field see e.g. [25]). The theoretical analysis provides the possibility to obtain detailed insight into the factors governing the catalyst activity and the stereocontrol of asymmetric reactions. In particular selectivity-determining interactions are of great interest in order to generate more selective chiral catalysts. These interactions are often of non-covalent character, including repulsive forces (sterics) but also attractive forces such as C-H/π dispersion type interactions, which are increasingly recognized as selectivity-determining factors (for a recent review on this topic see also [26]).[27,28,29,30]

Different iron-catalyzed hydrogenation reactions have been studied computationally,[31, 32] inluding the symmetric iron-cyclopentadienone-catalysed hydrogenation of acyclic imines [33,34] and ketones.[35,36] However, to our knowledge a similar analysis for iron–cyclopentadienone-catalysed hydrogenation in presence of a Brønsted acid has not yet been performed. As pointed out by Sunoj and coworkers,[24c] to date there are few computational transition state models of cooperative systems involving a transition metal and a Brønsted acid (a relevant study on cooperative palladium-catalyzed allylation was reported by Jindal and Sunoj[37]; for a recent review see [24c]). The factors governing the stereocontrol of iron-Brønsted-acid-catalysed asymmetric imine hydrogenations are currently unknown. We have here employed large quantum chemical models (up to 160 atoms) at the DFT-D level to evaluate the asymmetric hydrogenation of 2H-1,4-benoxazines with Knölker's complex in absence and in presence of chiral phosphoric acids (corresponding to the reaction in Figure 1).[22] A detailed mechanism is proposed, which is consistent with experimental observations reported by Zhou *et al.* on possible reaction intermediates.[20] The computed enantioselectivities with two different chiral phosphoric acid show excellent agreement with experimental values, allowing for the identification of interactions involved in the stereocontrol.

Results and Discussion

Knölker's complex is able to mediate hydrogenation of imines with molecular H_2 in presence and in absence of phosphoric acids.[14,15,22] The hydrogenation reaction comprises two essential parts: *i*) formation of the active catalyst species and *ii*) hydrogenation of the substrate. Experimental and computational results indicate that these two steps energetically and mechanistically might be very different in presence and absence of a phosphoric acid.[22,33] We have here evaluated the mechanistic details of catalyst activation and benzoxazine (**S1**) hydrogenation with Knölker's complex, in absence or presence of phosphoric acid (**P1** or **P2,** Figure 2) at the B3LYP-D2 and B3LYP-D3 level.

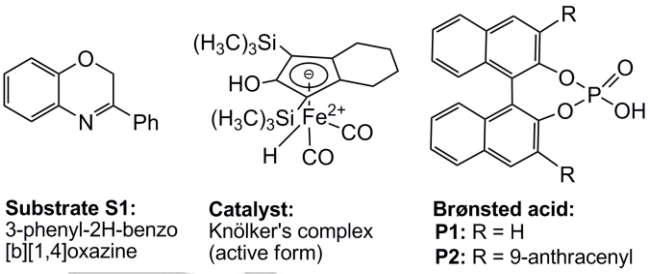

Figure 2. Systems studied here.

H_2 splitting and imine hydrogenation in absence of phosphoric acid

H_2 splitting: Knölker's complex as shown in Scheme 1 (**Fe(II)H,OH**) is considered the active hydrogenation species in absence of other additives.[14] This complex is bifunctional, with an Fe(II)-bound hydride and an acidic OH group on the cyclopentadienone ligand. During hydrogenation, the active catalyst species has to be continuously reformed. This formation has been studied computationally for a related iron complex by von der Höh and Berkessel.[33] A mechanism as shown in Scheme 1A was proposed, assuming the coordinatively unsaturated **Fe(0)** complex as initial species. After coordination of H_2 to the iron centre, a proton transfer from H_2 to the cyclopentadienone ligand occurs, forming the active complex (Scheme 1A). An analogue mechanism was computed here for Knölker's complex. The computed barrier for H_2 splitting is 17.9 kcal/mol relative to **Fe(0)** (singlet state) and free H_2 (23.5 kcal/mol relative to the H_2-coordinated intermediate, **Fe(0)-H2**, B3LYP-D2). The overall driving force for H_2 splitting then becomes -16.5 kcal/mol, making this step highly exergonic. A similar conclusion was reached by von der Höh and Berkessel.[33]

Interestingly, we find that the triplet state of the **Fe(0)** complex is 2.7 kcal/mol lower in energy than the singlet state. However, during the catalytic reaction it might be expected that the iron complex remains in the singlet state.

The above analysis related to H_2 splitting by Knölker's complex is only relevant to the experimental system if it is assumed that the coordinatively unsaturated **Fe(0)** complex will be formed under reaction conditions. This is here considered to be questionable, given that both imines and amines are present in the reaction mixture, both of which have high affinity for the iron centre. Under such conditions, we propose that the iron centre will be coordinated by the amine, resulting in a different

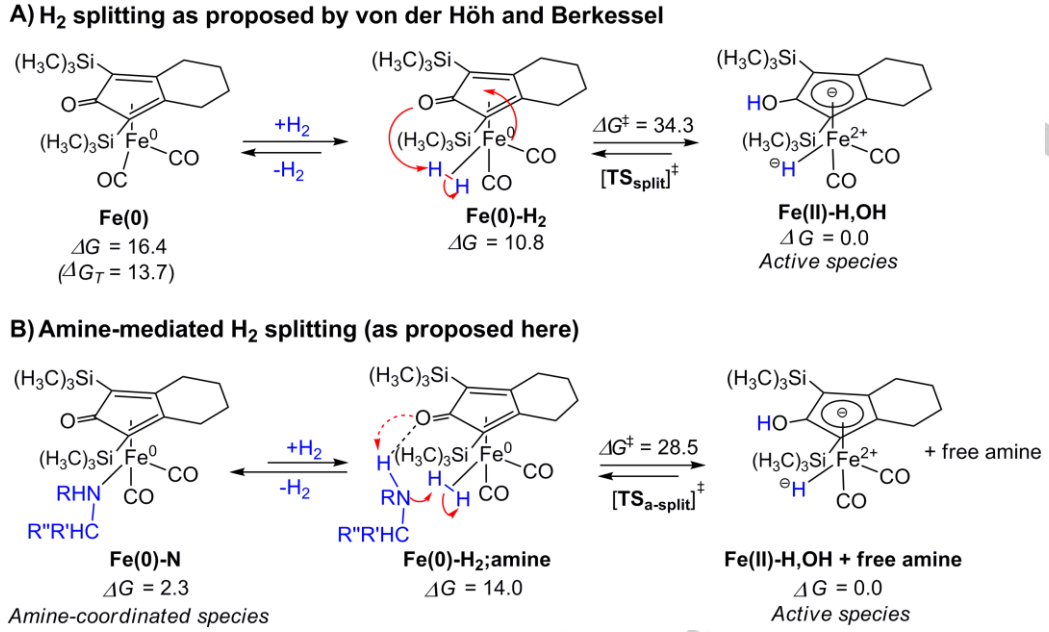

Scheme 1. H_2 splitting with Knölker's complex. **A)** Mechanism as proposed by von der Höh *et al.* for a related complex.[33] Free energies (333K, B3LYP-D2) as computed here are given relative to the resting state **Fe(II)-H,OH** (ΔG_T = triplet state). **B)** Mechanism for H_2 splitting as proposed here. During hydrogenation conditions, it is proposed that the amine product coordinates to the iron centre. H_2 splitting is mediated by the amine.

mechanism for formation of the active species and very different relative energies (Scheme 1B). Our proposal is in agreement with observations by Beller and co-workers that following formation of the amine product, the amine might coordinate to the iron centre.[20] Also for iron-mediated aldehyde and ketone hydrogenation, the formed alcohol product has been proposed to coordinate to the iron complex.[15,36,35] In our calculations, coordination of the amine is highly favourable (by around 14 kcal/mol), making the relative energy of the **Fe(0)-N** complex comparable to that of the resting state, **Fe(II)-H,OH.** Hence, in presence of amine, H_2 addition and splitting is only slightly exergonic (-2.3 kcal/mol, B3LYP-D2, Scheme 1B).

We further propose that the amine product might be involved in regenerating the active catalyst species by mediating the proton transfer to the cyclopentadienone ligand (Scheme 1B). This is analogue to the proposal by Casey and Guan that under ketone hydrogenation conditions, the alcohol product is involved in H_2 activation.[15] In our calculations, the barrier for amine-mediated proton abstraction from H_2 is around 6 kcal/mol smaller than direct transfer (Scheme 1). The heterolytic H_2 cleavage mediated by the amine is reminiscient of a 'frustrated Lewis pair' mechanism for H_2 splitting, where the amine acts as a Lewis base and the **Fe(0)-H₂** complex acts as the Lewis acid.[38] The proton transfer is followed by a spontaneous proton delivery to the oxygen atom of the cyclopentadienone ligand, yielding the active species **Fe(II)-H,OH**. A similar amine-assisted protonation of a ligand has been proposed by Oro and co-workers for a half-sandwich iridium(III) complex. [39]

In summary, we suggest that the previously proposed mechanism for H_2 splitting by a Knölker's type complex (in absence of additives such as phosphoric acid)[33] should be modified on several points. First, during imine hydrogenation conditions, it is proposed that an unsaturated **Fe(0)** species does not form, but instead the amine-coordinated species (**Fe(0)-N**). From here, H_2 splitting and uptake is slightly exergonic. Second, H_2 splitting is proposed to be assisted by the amine product.

Imine hydrogenation: The (symmetric) hydrogenation mechanism of a Knölker's type complex with an acyclic imine substrate has been studied computationally by von der Höh and Berkessel,[33] and by Moulin and co-workers.[34] Also for the conceptually related ruthenium complex (Shvo's catalys), the imine hydrogenation mechanism has been studied theoretically.[40] Additionally, computational studies of aldehyde hydrogenation with Knölker's complex have been reported.[35] To our knowledge, the hydrogenation mechanism of a cyclic imine such as **S1** with Knölker's complex has not been evaluated theoertically previously. We have therefore studied this mechanism here in order to analyze the differences between benzoxazine hydrogenation mechanisms in presence and absence of Brønsted acid.

The imine hydrogenation pathway reported by von der Höh and Berkessel for a Knölker's type complex comprises a bifunctional outer sphere mechanism, involving step-wise proton transfer from the OH group of the ligand and hydride transfer from the iron complex to the acyclic imine (Scheme 2).[33] Related bifunctional outer sphere imine hydrogenation mechanisms have been proposed for e.g. iridium catalysts.[41, 42] We have here attempted to compute the mechanism shown in

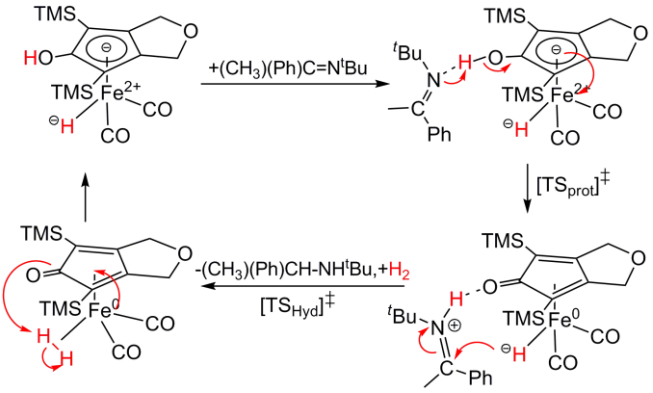

Scheme 2. Mechanism proposed by von der Höh and Berkessel for hydrogenation of acyclic imines with a Knölker's type complex (drawn here on basis of the computed results given in ref. [33]).

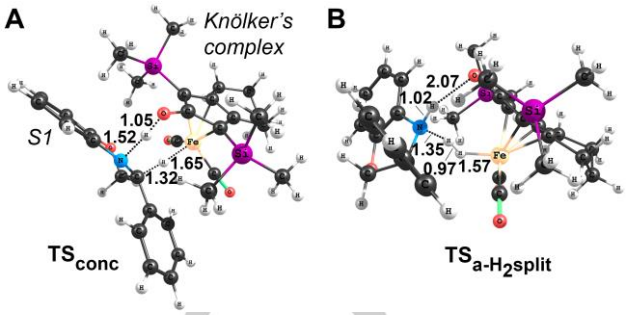

Figure 3. Optimized transition state geometries (B3LYP-D2) for concerted proton and hydride transfer to **S1** (A) and for amine-assisted H_2 splitting (B, see Scheme 3 for full mechanism).

Scheme 2 with Knölker's complex and benzoxazine **S1** (3-phenyl-2H-benzo[b][1,4]oxazine, Figure 2) at the B3LYP-D2 level. Our results show several differences to the mechanism in Scheme 2. Mainly, we find that hydrogenation of benzoxazine with Knölker's complex (in absence of additives) occurs through a single concerted transition state involving simultaneous proton and hydride transfer to the imine (Scheme 3, Figure 3). This is in line with computational results by Moulin *et al.* for concerted iron-mediated hydrogenation of an acyclic imine formed during reductive amination,[34] and by Lu *et al.* for concerted iron-mediated aldehyde hydrogenation.[35] Although imine hydrogenations often are proposed to occur through stepwise proton and hydride transfer, [29,39,43] also concerted mechanisms have been proposed for some bifunctional iridium-based and ruthenium-based systems. [39,40,41] The concerted mechanism is also reminiscent of the bifunctional mechanism proposed for ruthenium-mediated ketone hydrogenation. [44,45]

The barrier for the concerted imine hydrogenation is 22.3 kcal/mol (333 K), relative to the resting state (**Fe(II)-H,OH,** Scheme 3, B3LYP-D2). The amine product interacts through an agostic bond with the Fe-centre (with relative energy of 12.6 kcal/mol), but can then rearrange to coordinate through the nitrogen atom (**Fe(0)-N**). The amine-coordinated structure is located at -5.8 kcal/mol relative to the reactant complex **Fe(II)-H,OH** and free imine, which corresponds to the free energy change of imine to amine conversion (-8.1 kcal/mol) and the energy of the **Fe(0)-N** complex relative to **Fe(II)-H,OH** (2.3 kcal/mol, Scheme 1). The **Fe(II)-H,OH** complex has to be regenerated prior to a new hydrogenation cycle, with a computed barrier for amine-assisted H_2-splitting of 20.4 kcal/mol relative to **Fe(II)-H,OH** and free imine (Scheme 3).

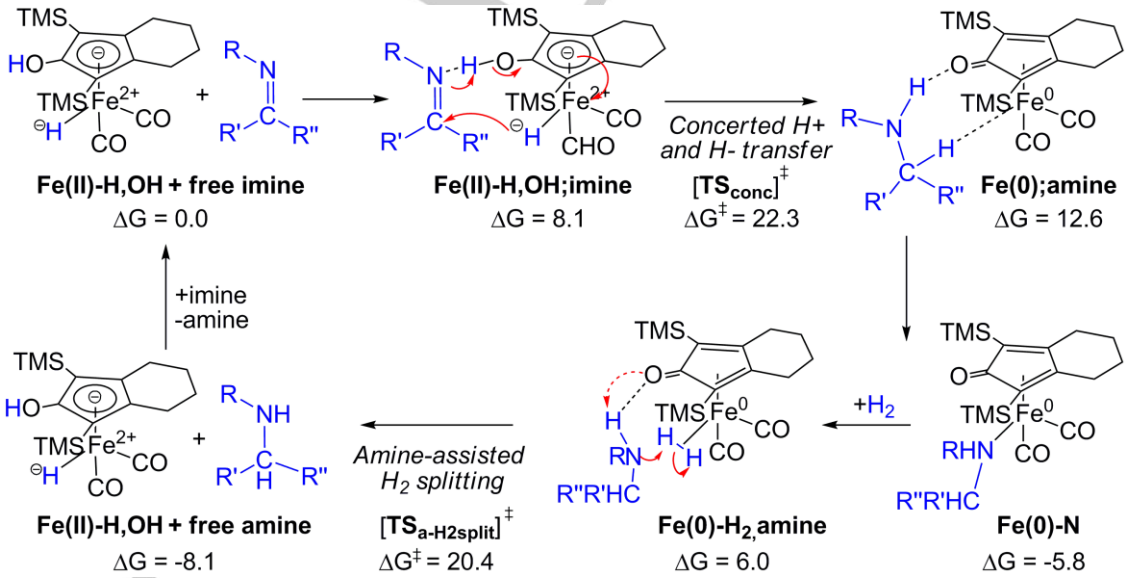

Scheme 3. Mechanism as proposed here for benzoxazine hydrogenation with Knölker's complex (free energies in kcal/mol, 333 K, B3LYP-D2, relative to **Fe(II)H,OH** plus free imine **S1**).

H_2 splitting and imine hydrogenation in presence of phosphoric acid

H_2 splitting in presence of phosphoric acid: The uptake of H_2 by Knölker's complex can be expected to be mechanistically and energetically different in presence of an additive such as a Brønsted acid. Beller and co-workers have shown that addition of phosphoric acid to Knölker's complex results in release of H_2.[20] It was proposed that this is due to formation of a phosphoric acid-iron adduct, where the acid coordinates through an oxygen atom (Scheme 4, **Fe(II)-P,OH**).[20] These experimental results indicate that in presence of Brønsted acid, the resting state of the system is the adduct **Fe(II)-P,OH**, with H_2 uptake expected to be endergonic, in contrast to the slightly exergonic process computed in absence of phosphoric acid (Scheme 1B). The computational analysis support this scenario. We find that the adduct **Fe(II)-P,OH** lies low in energy, with a cost of 21.6 kcal/mol for cleavage of the Fe-O(P) bond and coordination of H_2 (Scheme 4, B3LYP-D2). From here, H_2 splitting is facile, with a TS barrier of 22.7 kcal/mol relative to **Fe(II)-P,OH**. The species formed, **Fe(II)-H,OH-PH**, is proposed to be the active catalyst. Formation of **Fe(II)-H,OH-PH** is indeed highly endergonic (15 kcal/mol), explaining why addition of phosphoric acid to Knölker's complex results in release of H_2.[20] Note also that the electronic description of the resting state adduct is someone different than that proposed by Beller and co-workers.[20] Beller's proposal indicates a Fe(0) description, with the proton residing on the phosphoric acid,[20] whereas the computations performed here indicate that the iron has oxidation state (II) in the adduct, with the proton residing on the cyclopentadienone ligand (Scheme 4, **Fe(II)-P,OH**).

Hydrogenation mechanism in presence of phosphoric acid: In presence of a chiral Brønsted acid and Knölker's complex, asymmetric hydrogenation of benzoxazines is observed.[22] A direct interaction of the chiral acid with the substrate or the iron-complex is required, as the experimentally observed enantioselectivity otherwise cannot be explained. To our knowledge, computational studies of the imine hydrogenation mechanism with Knölker's complex in presence of a phosphoric acid have not been reported previously. However, a mechanistic proposal (not involving any computations) for hydrogenation of acyclic imines has been given in the dissertation of Zhou (Scheme 5).[46] In Zhou's proposal, the acid and the imine complexate, followed by formation of a three-membered supramolecular complex, in which both Knölker's catalyst and the imine are hydrogen-bonded to the phosphoric acid. Concerted proton transfer from the acid and hydride transfer from the iron centre give the amine product, which coordinates to the iron through the nitrogen atom. Release of the amine results in formation of the phosphoric acid-iron adduct. According to the proposal by Zhou, addition of H_2 results in complete release of the acid and no further interaction with the iron complex (Scheme 5).[46]

We have here studied the hydrogenation mechanism of imine **S1** with Knölker's complex in presence of phosphoric acid **P1**. On basis of these calculations, we propose a different

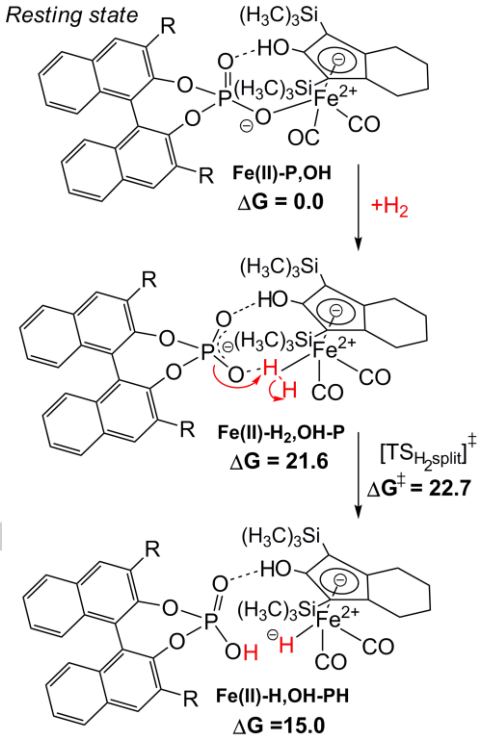

Scheme 4. H_2 splitting with Knölker's complex in presence of additive **P1** (R = H, free energies in kcal/mol, 333 K, B3LYP-D2).

mechanism than Zhou. Firstly, we predict that a hydrogen-bonded interaction between the phosphoric acid and Knölker's complex remains constants throughout the catalytic cycle. Therefore, in our mechanism, H_2 splitting occurs through abstraction of a proton by the phosphoric acid (Scheme 6). The imine molecule interacts with the **Fe(II)-H,OH-PH** structure through a hydrogen-bond. Transfer of a proton from the phosphoric acid to the imine has a very low barrier (12.6 kcal/mol, B3LYP-D2), which is underestimated in calculations (underestimation of low-barrier proton transfer steps has been observed in other systems).[47,48] In a second step, hydride transfer occurs, with a barrier of 17.2 kcal/mol (given relative to the resting state, B3LYP-D2). At the preferred pro-(*S*) transition state for hydride transfer, the Brønsted acid **P1** has only one oxygen involved in hydrogen bond interactions with the substrate and the iron complex, whereas the second oxygen makes a C-H…O interaction with the *ortho*-hydrogen of the phenyl substituent of **S1** (Scheme 6). Alternative conformations involving both oxygen atoms in hydrogen-bonding interactions are >4 kcal/mol higher in energy.

The amine formed immediately after hydride transfer has an agostic interaction between the amine proton and the iron centre, however, as discussed above, coordination of the amine to the iron centre is strongly favourable. The energy of the product complex is 5.5 kcal/mol relative to the resting state, however, the overall driving force for conversion of **S1** to the corresponding amine is computed to be -8.1 kcal/mol.

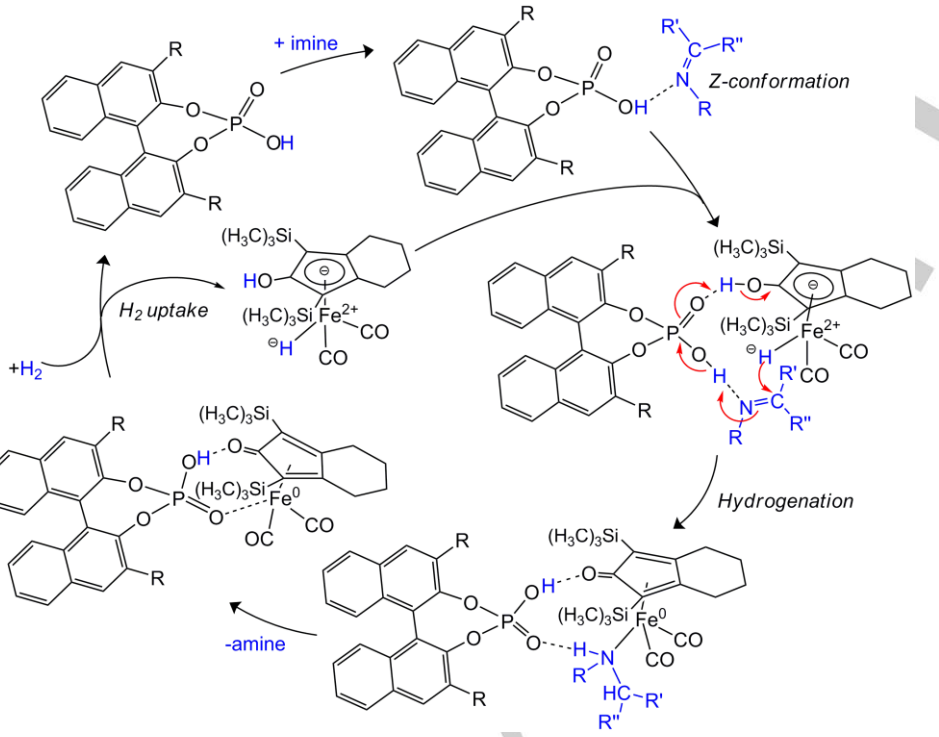

Scheme 5. Mechanism proposed by Zhou for hydrogenation of acyclic imines with Knölker's complex in presence of phosphoric acid (adapted from [46]). Formal charges are indicated to clearly illustrate the flow of electrons.

The computed results for iron-phosphoric acid mediated imine hydrogenation indicate that hydrogenation is not a concerted process but occurs stepwise. A TS for concerted proton and hydride transfer as proposed by Zhou (Scheme 5) [46] could not be located in computations. Constrained geometry optimization of a concerted TS (with frozen scissile bond distances estimated from the concerted TS obtained in absence of phosphoric acid, Scheme 3) provides an approximate barrier of 31 kcal/mol for a concerted TS. This value is 14 kcal/mol above the stepwise hydrogenation (Scheme 6), making a concerted mechanism as shown in Figure 5 unlikely. It can further be noted that in the mechanism proposed here (Scheme 6), the iron oxidation state (+2) and formal charge assignment of the cyclopentadienone ligand (-1) remain constant throughout the cycle. This is in contrast to the proposal by Zhou, where the iron oxidation states alternates between 0 and +2 (Scheme 5).

The computed energies show that the rate-limiting step for the mechanism proposed in Scheme 6 is H_2 splitting (22.7 kcal/mol, B3LYP-D2, Scheme 6). Computations with B3LYP-D3 show relative energies that differ up to 2.2 kcal/mol relative to B3LYP-D2, but do provide the same energetic trend, with barriers of 21.4 kcal/mol for H_2 splitting and 18.5 kcal/mol for hydride transfer (SI, Table S1). Calculation of the critical steps with acid **P2** also provide a similar picture. With **P2**, the barrier for H_2 splitting is 20.4 kcal/mol (B3LYP-D2), whereas the lowest-lying hydride transfer transition state has a barrier of 17.0 kcal/mol.

Enantioselectivity of benzoxazine hydrogenation

We have computed the diastereomeric transition states for iron-mediated hydrogenation of substrate **S1** in presence of two different chiral Brønsted acids, **P1** or **P2** (Figure 2, see Supporting Information (SI) for optimized geometries). These calculations are challenging due to the size and the flexibility of the iron complex and the Brønsted acid. Knölker's complex features a fused ring system as ligand, with the cyclohexyl part adopting a half-chair conformation in the optimized structures. A half-chair of this kind can exhibit different helicities (Figure 4). This is of less relevance for the free iron complex (as the complex is symmetric, the two helicities have the same energy). However, for the chiral Brønsted-acid-coordinated complex, the two helicities show slightly different energies. Therefore, all TS geometries were located for both helicities.

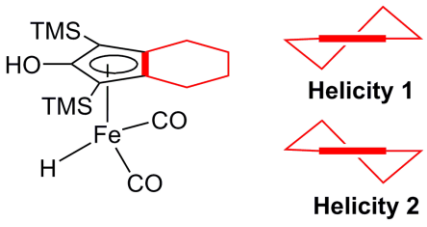

Figure 4. The half-chair conformation of the fused cyclohexyl ring of Knölker's complex can adopt two different helicities.

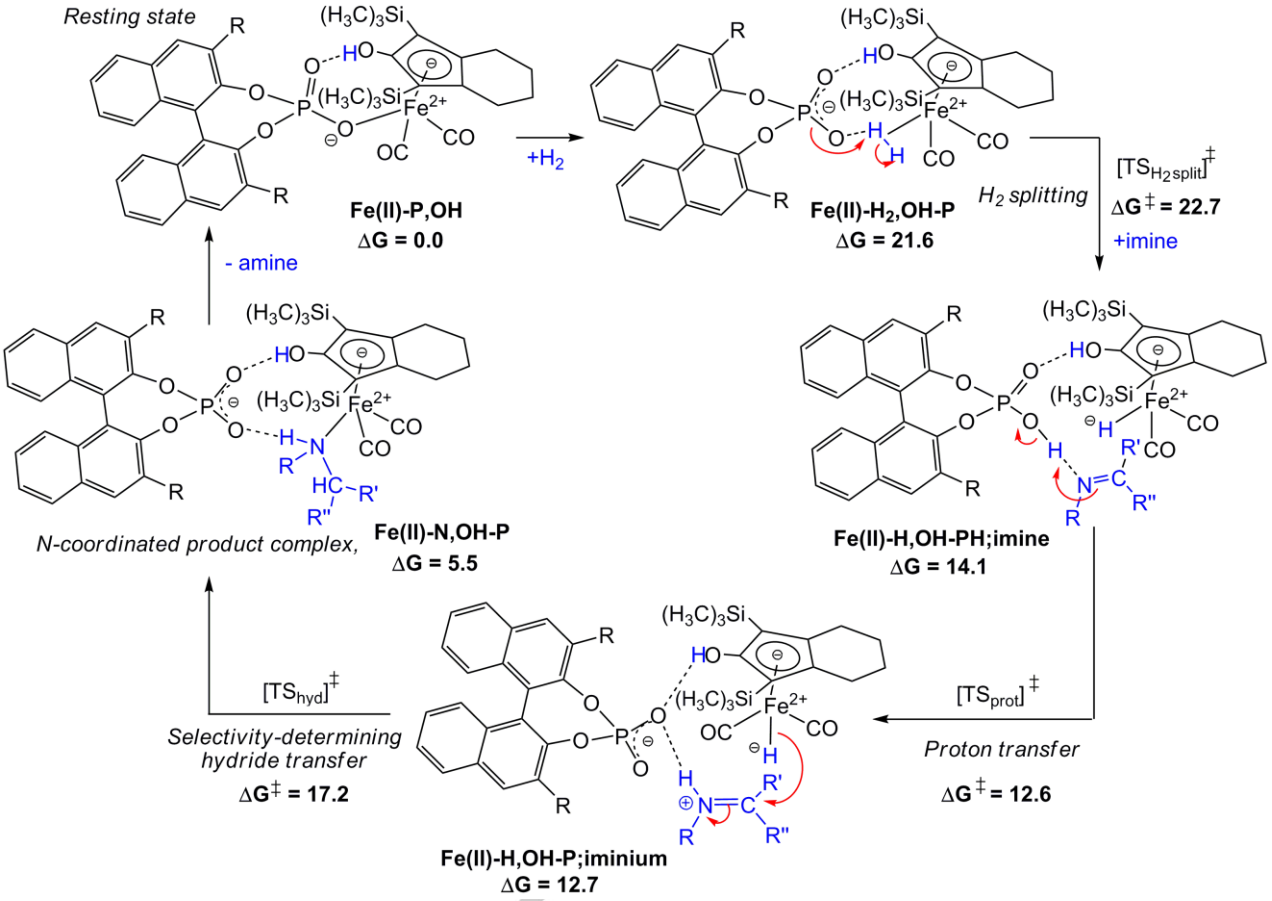

Scheme 6. Mechanism proposed here for imine hydrogenation mediated by Knölker's complex in presence of phosphoric acid (computed with R = H, free energies in kcal/mol, 333 K, B3LYP-D2). Formal charges are indicated to clearly illustrate the flow of electrons.

The two lowest-lying diastereomeric TS structures for **P1**-iron-mediated hydrogenation of **S1** are given in Figure 5. The calculations shows that the pro-(*R*) and pro-(*S*) pathways in helicity 1 have similar energies (Table 1, B3LYP-D2), however, for helicity 2, the pro-(*S*) pathway is less favourable. The computed energies lead to a ratio of 27(S):73(*R*), which is somewhat different from the experimental ratio (52(S):48(*R*)[22]). However, it can be noted that the deviation from experiment roughly corresponds to a too large barrier for the lowest-lying TS of 0.6 kcal/mol, i.e. the error of B3LYP-D2 is not large in energetic terms. Interestingly, for B3LYP-D3, the ΔΔG≠ values are slightly different, leading to a switch in major product enantiomer. The computed ratio is 48(R):52(S), which is identical to the experimental distribution, indicating that B3LYP-D3 provides a better description of the selectivity-determining interactions of this system. The perfect match with the experimental ratio should be considered fortuitous though.

For **P2**-assisted hydrogenation, the conformational analysis reveals two energetically low-lying orientations of the Brønsted acid with respect to the iron complex: the 9-anthracenyl substituents of **P2** can either lie above and below the iron complex (orientation **A**, Figure 6) or perpendicular to this orientation, with the 9-anthracenyl substituents placed left and right of the complex (orientation **B**, Figure 6). In both orientations two oxygen atoms of **P2** are involved in hydrogen bonds with the substrate and iron complex. Alternative orientations involving only one oxygen atom in the hydrogen-bonding network (corresponding to the preferred conformation with acid **P1**, Scheme 3) were found to lie higher in energy.

Table 1. Computed ΔΔG≠ values (333 K) for diastereromeric TS structures for **P1**-iron-mediated hydrogenation of **S1**.[a]

	Stereo	Heli-city[b]	B3LYP-D2[c] ΔΔG≠	B3LYP-D3[c] ΔΔG≠	Exp.[d]
P1-TS$_{hyd}$**I**	*pro-(R)*	1	**0.0**	0.3	
P1-TS$_{hyd}$**II**	*pro-(R)*	2	0.2	0.4	
P1-TS$_{hyd}$**III**	*pro-(S)*	1	0.3	**0.0**	
P1-TS$_{hyd}$**IV**	*pro-(S)*	2	1.7	1.1	
(*S*):(*R*)			27:73[e]	52:48[e]	52:48

[a]See Figure 2 for **P1** and **S1**, [b]See Figure 4. [c]Energies given relative to lowest lying TS at each level of theory. [d]Experimental, from [22].[e]The ratios are computed based on all TS energies (I to IV).

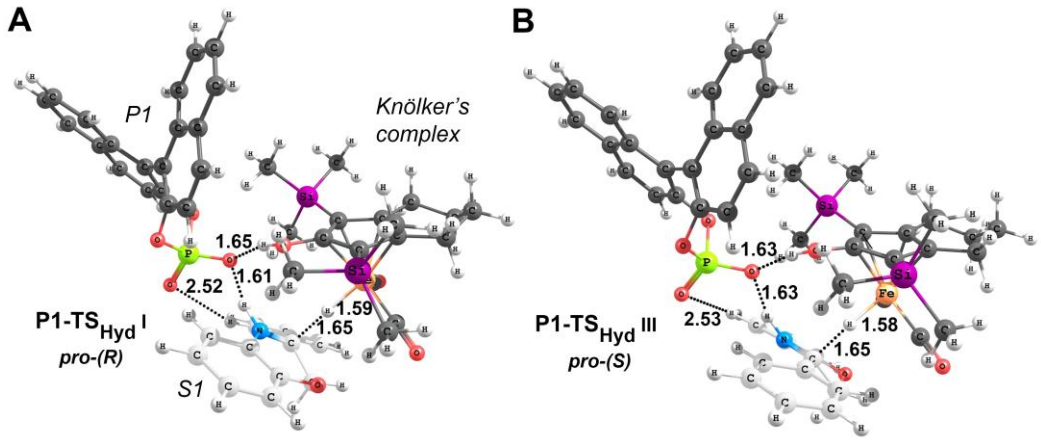

Figure 5. Two lowest-lying diastereomeric hydride transfer TS structures for **P1**-iron-mediated hydrogenation of **S1**, **A) P1**-TS$_{hyd}$**I**, pro-(*R*), **B) P1**-TS$_{hyd}$**III**, pro-(*S*) (both in helicity 1, B3LYP-D3). Substrate carbon atoms shown in grey. For energies, see Table 1. For full mechanism see Scheme 6.

Interestingly, conformations **A** and **B** are similar in energy for the pro-(*R*) transition states (especially at the B3LYP-D3 level), whereas for the pro-(*S*) transition states, conformation **A** is clearly preferred (Table 2). The lowest-lying pro-(*R*) and pro-(*S*) TS geometries for **P2**-iron-mediated hydrogenation of **S1** are given in Figure 7. For the enantiomeric product ratio of **P2**-assisted hydrogenation, B3LYP-D3 again provides somewhat better results than B3LYP-D2 (Table 2). The deviation from experiment is roughly 0.1 kcal/mol for D3 and 0.6 kcal/mol for D2. As for **P1**, the excellent agreement between experiment and B3LYP-D3 computations should be considered fortuitous.

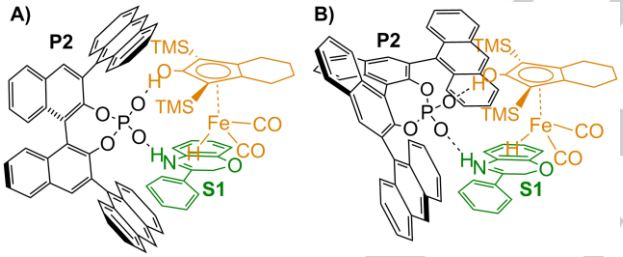

Figure 6. Possible orientations (**A** and **B**) of Brønsted acid **P2** when hydrogen-bonded to Knölker's complex and **S1**.

Selectivity-determining interactions

The interactions between the Brønsted acid, the substrate and Knölker's complex determine the enantioselectivity of the reaction (assuming that the solvent, toluene, is not involved in relevant interactions).

The orientation of the phosphoric acid **P1** is mainly governed by hydrogen bond interactions between the phosphate oxygen atoms, the OH ligand of the iron complex and the NH-moiety of the iminium (Figure 8A). Additionally there are dispersion type C-H/π interactions between the Si-CH$_3$ groups and the π -system of **P1**, as well with the substrate π system. Various C-H…O(P) interactions can be identified: between the phosphate oxygen and an *ortho*-hydrogen on the phenyl substituent of **S1** and the related hydrogen on the fused ring system of **S1**, as well as related C-H…O=C interactions between the carbonyl ligands and the *ortho*-hydrogen of the phenyl substituent and the CH$_2$ group on the ring of **S1** (Figure 8A). The C-H…O interactions to the phosphate and the C=O show the main differences between **P1**-TS$_{hyd}$**I** and **P1**-TS$_{hyd}$**III**, with stronger interactions observed for the preferred (*S*)-forming TS (Table 3).

The selectivity-determining interactions for **P2** are of the same type. For **P2**, dispersion interactions between the 9-anthracenyl substituents and Knölker's complex and the substrate are also relevant (Figure 8B). In orientation **A**, these are mainly C-H/π interactions between Si-CH$_3$ and 9-anthracenyl, in orientation **B** also C-H/π interactions between 9-anthracenyl and the substrate are observed.

Table 2. Computed $\Delta\Delta G^{\neq}$ values (333 K) for diastereromeric TS structures for **P2**-iron-mediated hydrogenation of **S1**.[a]

	Stereo	Heli-city[b]	Orien-tation[c]	B3LYP-D2[c] $\Delta\Delta G^{\neq}$	B3LYP-D3[c] $\Delta\Delta G^{\neq}$	Exp. [e]
P2-TS$_{hyd}$**I**	*pro-(R)*	1	A	0.4	1.0	
P2-TS$_{hyd}$**II**	*pro-(R)*	2	A	0.1	1.2	
P2-TS$_{hyd}$**III**	*pro-(R)*	1	B	2.1	1.4	
P2-TS$_{hyd}$**IV**	*pro-(R)*	2	B	1.3	1.3	
P2-TS$_{hyd}$**V**	*pro-(S)*	1	A	0.7	0.8	
P2-TS$_{hyd}$**VI**	*pro-(S)*	2	A	**0.0**	**0.0**	
P2-TS$_{hyd}$**VII**	*pro-(S)*	1	B	4.2	4.9	
P2-TS$_{hyd}$**VIII**	*pro-(S)*	2	B	4.2	4.7	
(*S*):(*R*)				46:54[e]	70:30[e]	66:33

[a]See Figure 2 for **P2** and **S1**, [b]See Figure 4,[c]See Figure 6, [d]Energies given relative to lowest lying TS at each level of theory. [e]Experimental, from [22].].[e]The ratios are computed based on all TS energies (I to VIII).

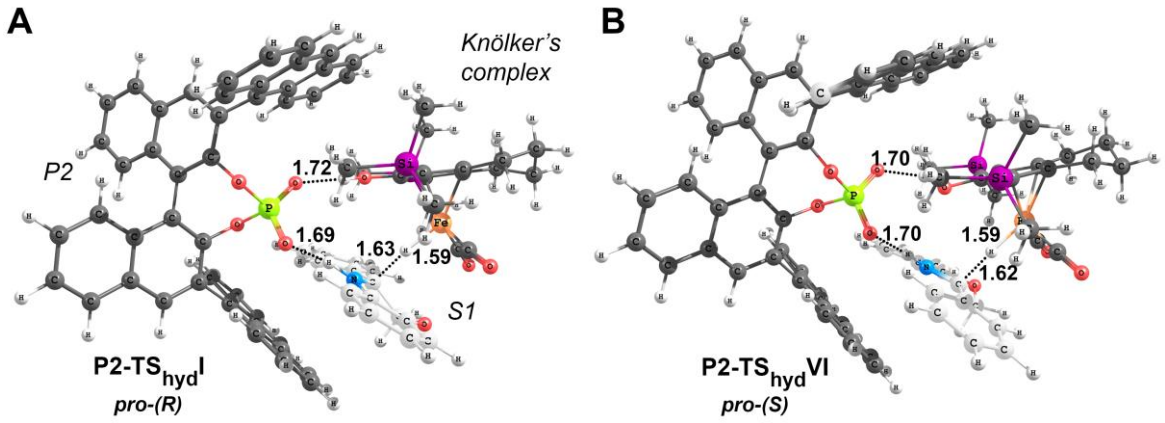

Figure 7. The lowest-lying pro-(*R*) and pro-(*S*) hydride transfer TS geometries for **P2**-iron-mediated hydrogenation of **S1, A) P2**-TS$_{hyd}$**I,** pro-(*R*), helicity 1, orientation A, **B) P2**-TS$_{hyd}$**VI**, pro-(*S*), helicity 2, orientation A (B3LYP-D3). Substrate carbon atoms shown in grey. For energies see Table 2.

Table 3. Selected distances (B3LYP-D3) at the lowest lying diastereomeric transition states for **P1-** and **P2**-iron-mediated hydrogenation of **S1**.

		Distances (Å) [a]						
TS	***Stereo***	***C-H$_{ortho}$ …(P)O***	***C-H$_{fused}$ …(P)O***	***O-H …(P)O***	***N-H …(P)O***	***C-H$_{ortho}$ …O=C***	***HC-H$_{fused}$ …O=C***	**$\Delta\Delta G^{\neq}$**
P1-TS$_{hyd}$**I**	*pro-(R)*	2.52	3.52	1.65	1.61	2.87	2.81	0.3
P1-TS$_{hyd}$**III**	*pro-(S)*	3.20	2.53	1.63	1.63	2.71	2.79	**0.0**
P2-TS$_{hyd}$**I**	*pro-(R)*	2.46	2.27	1.72	1.69	2.90	3.26	1.0
P2-TS$_{hyd}$**VI**	*pro-(S)*	2.10	2.63	1.70	1.70	2.85	3.26	**0.0**

[a]See also Figure 8 for illustration of relevant distances. C-H$_{ortho}$= H on *ortho*-C of Ph substituent of **S1** , C-H$_{fused}$ = H on C of fused ring of **S1** , O-H = OH group on cyclopentadienone, N-H= NH group of **S1** (iminium form), HC-H$_{fused}$ = H on CH_2 of fused ring of **S1.**

Comparison of the lowest-lying hydride-transfer transition state for formation of the (*R*)-amine (**P2**-TS$_{hyd}$**I**) and the (*S*)-amine (**P2**-TS$_{hyd}$**VI,** B3LYP-D3, Figure 7) shows that the type of interactions at the two TS geometries is fairly similar. The hydrogen bonds between the phosphate oxygen atoms and the substrate NH and the OH of the iron complex are also similar in lengths for **P2**-TS$_{hyd}$**I** and **P2**-TS$_{hyd}$**VI** (Table 3). The C-H…O interactions are again stronger at the preferred (*S*)-forming TS, which exhibits a relatively short interaction of 2.10 Å. C-H…O interactions thus appear to be essential for the stereocontrol of iron-Brønsted-acid catalyzed hydrogenation **S1**. Similar results have been obtained for other asymmetric systems, e.g. a related C-H…O interaction between a chiral phosphoric acid and the triphenyl phosphine ligand of a transition-metal catalyst was identified to be involved in the stereocontrol of cooperative palladium–catalyzed asymmetric allylation.[37] A C-H…O interaction was also identified as selectivity-determining interaction in proline-catalyzed intramolecular aldol reactions.[25d]

Conclusions

The mechanism for imine hydrogenation with Knölker's complex in absence and in presence of chiral phosphoric acids was investigated computationally. For the benzoxazine substrate **S1**, the computed hydrogenation mechanism with Knölker's complex (Scheme 3) differs from a previous proposal by von der Höh and Berkessel for a related iron complex with an acyclic imine.[34] This might be due to differences in the substrate. We find a concerted hydrogenation mechanism, followed by an amine-mediated proton transfer to regenerate the active catalyst complex.

In presence of phosphoric acid, the hydrogenation mechanism changes (Scheme 6). The resting state of the system is in this case an adduct between the iron complex and the deprotonated acid, in agreement with experimental observations.[20] H_2 splitting involves the phosphoric acid and is rate-limiting. Our calculations further indicate that hydrogenation occurs through a step-wise mechanism, where the phosphoric acid acts as the proton donor. This implies that the cyclopentadienone ligand and the iron complex do not change oxidation state during the catalytic cycle. Hydride transfer is the final step, with the position of the substrate dictated through interactions with the acid.

The phosphoric acid coordinates through an oxygen atom to the iron center in the resting state, but this interaction is broken during the catalytic cycle. The effect of the Brønsted acid on the stereocontrol is thus mediated through non-covalent interactions only. This is analogous to the proposal by Xiao, Iggo, and coworkers for cooperative iridium-catalyzed

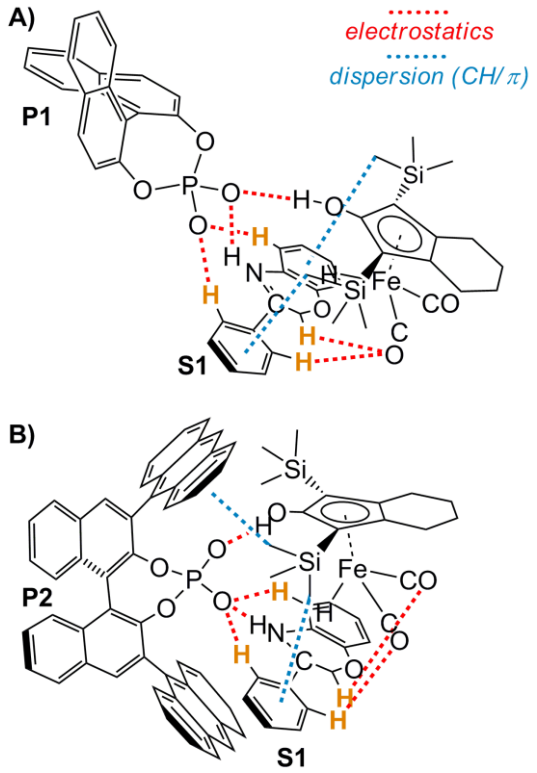

Figure 8. Illustration of selected non-covalent interactions at the selectivity-determining hydride-transfer transition state. **A**) Lowest lying TS with **P1** (**P1**-TS_{hyd} **III,** pro-(*S*)), **B**) Lowest lying TS with **P2** (**P2**-TS_{hyd}**VI,** pro-(*S*)). The hydrogens involved in C-H…O interactions are high-lighted in orange.

asymmetric imine hydrogenation,[49] and by Sunoj and coworkers for cooperative palladium-catalyzed asymmetric allylation.[37] For the iron-Brønsted acid system investigated here, the selectivity-determining interactions include electrostatic and dispersion interactions. C-H…O interactions appear particularly relevant (Figure 8, Table 3). The calculated enantiomeric ratios show very good agreement with experiment, with B3LYP-D3 showing slightly better results than B3LYP-D2 (Table 1 and 2).

Computational Section

Models: Calculations were performed with full models of Knölker's catalyst, the chiral phosphoric acids and the imine substrate (Figure 2). Models with **P1** have a size of 116 atoms, those with **P2** comprise 160 atoms. All calculations were performed with a singlet electronic state, unless otherwise indicated. Triplet states were explicitly evaluated, as described in the text. Optimized coordinates for the mechanisms proposed in Scheme 3 and Scheme 6, as well as of the diastereomeric transition states structures with **P1** and **P2** are given in the SI.

Methods: All computations were performed using the hybrid density functional B3LYP[50] as implemented in revision D.01 of the Gaussian 09 package.[51] The implicit solvent model IEFPCM[52] (toluene, including only the electrostatic terms) and the Grimme empirical dispersion correction D2[53] were included in optimization of all geometries (additional calculations were performed with the dispersion correction D3[54] instead of D2, see main text). Convergence criteria were tightened as opt=tight. The basis set 6-311G(d,p) was employed on all atoms in geometry optimizations, followed by single point calculations employing 6-311+G(2d,2p) to obtain more accurate electronic energies. Thermochemical quantities were obtained from frequency calculations at the same level of theory as the geometry optimizations, with temperature corrections to adjust for the experimental temperatures (333 K[22]). Counterpoise corrections were computed for all systems at the higher basis set level. All reported energies are Gibbs free energies (kcal/mol), corresponding to a standard state of 1 atm (0.041 M) for all species. If the pressure of H_2 is adjusted to 5 bar (4.93 atm) in calculations, all relative energies are reduced by 1.1 kcal/mol. The computed enantiomeric ratios are not affected by standard state conversions or changes of the pressure in calculations.

Acknowledgements

This work has been supported by the Research Council of Norway through a FRIPRO grant (No. 231706/F20) to K. H. Hopmann, through a Centre of Excellence Grant (No. 179568/V30), and by the Norwegian Supercomputing Program (NOTUR) through a grant of computer time (No. nn9330k).

Keywords: Asymmetric hydrogenation • Iron • Enantioselectivity • Brønsted acid • Imine

Entry for the Table of Contents

FULL PAPER

The mechanism and strereocontrol of iron-Brønsted-acid-catalysed asymmetric hydrogenation of benzoxazines is investigated using DFT-D methods and models of up to 160 atoms. Excellent agreement with experimental enantiomeric ratios indicates that DFT-D is able to correctly capture the selectivity-determining interactions, which are goverend by C-H…O attractions.

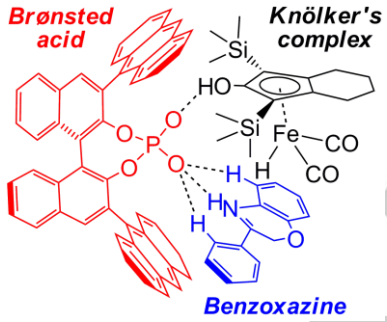

*Kathrin H. Hopmann**

Page No. – Page No.

Title

Iron-Brønsted-acid-catalysed asymmetric hydrogenation:

Mechanism and selectivity-determining interactions

References

[1] P. Etayo, A. Vidal-Ferran, *Chem. Soc. Rev.* **2013**, *42*, 728-754.

[2] D. J. Ager, D. J.; de Vries, A. H. M.; de Vries, J. G. *Chem. Soc. Rev.* **2012**, *41*, 3340-3380.

[3] K. H. Hopmann, A. Bayer, *Coord. Chem. Rev.* **2014**, *268* , 59-82.

[4] R. Noyori, T. Ohkuma, T. *Angew. Chem., Int. Ed.Engl.* **2001**, *40*, 40-73.

[5] R. M. Bullock (*Ed*) *Catalysis without precious metals*, Wiley-VCH, Hoboken, NJ, **2010**.

[6] G. Zhang, B. L. Scott, S. K. Hanson, *Angew. Chem. Int. Ed.* **2012**, *51*, 12102-12106.

[7] G. Zhang, K. V. Vasudevan, B. L. Scott, S. K. Hanson, *J. Am. Chem. Soc.* **2013**, *135*, 8668−8681.

[8] S. Monfette, Z. R. Turner, S. P. Semproni, P. J. Chirik, *J. Am. Chem. Soc*. **2012**, *134*, 4561-4564.

[9] M. R. Friedfeld, M. Shevlin, J. M. Hoyt, S. W. Krska, M. T. Tudge, P. J. Chirik *Science* **2013**, *342,* 1076-1080.

[10] R. Langer, G. Leitus, Y. Ben-David, D. Milstein, *Angew. Chem., Int. Ed.* **2011**, *50*, 2120−2124.

[11] R. Langer, M. A. Iron, L. Konstantinovski, Y. Diskin-Posner, G. Leitus, Y. Ben-David, D. Milstein, *Chem. Eur. J.* **2012**, *18*, 7196−7209.

[12] C. Sui-Seng, F. Freutel, A. J. Lough, R. H. Morris, *Angew. Chem., Int. Ed.* **2008**, *47*, 940−943.

[13] P. O. Lagaditis, P. E. Sues, J. F. Sonnenberg, K. Yang Wan, A. J. Lough, R. H. Morris, *J. Am. Chem. Soc*. **2014**, *136*, 1367−1380

[14] C. P. Casey, H. Guan *J. Am. Chem. Soc.* **2007**, *129*, 5816-5817.

[15] C.P. Casey, H. Guan, *J. Am. Chem. Soc.* **2009**, *131*, 2499-2507.

[16] A. Berkessel, S. Reichau, A. von der Höh, N. Leconte, J.-M. Neudörfl, *Organometallics* **2011**, *30*, 3880−3887.

[17] A. Quintard, J. Rodriguez, *Angew. Chem. Int. Ed.* **2014**, *53*, 4044 – 4055.

[18] D. Parmar, E. Sugiono, S. Raja, M. Rueping, *Chem. Rev.*, **2014**, *114,* 9047–9153.

[19] M. Raynal, P. Ballester, A. Vidal-Ferran P. W. N. M. van Leeuwen, *Chem. Soc. Rev.* **2014**, *43*, 1660-1733

[20] S. Zhou, S. Fleischer, K. Junge, M. Beller, *Angew. Chem., Int. Ed.* **2011**, *50*, 5120−5124.

[21] S. Fleischer, S. Werkmeister, S. Zhou, K. Junge, M. Beller, *Chem. Eur. J.* **2012**, *18*, 9005−9010.

[22] S. Fleischer, S. Zhou, S. Werkmeister, K. Junge, M. Beller, *Chem. Eur. J.* **2013**, *19*, 4997 – 5003.

[23] J. L. Núñez-Rico, A. Vidal-Ferran, *Org. Lett.*, **2013**, *15*, 2066–2069.

[24] a) D. Balcells, F. Maseras, *New J. Chem.* **2007**, *31*, 333–343.; b) K. H. Hopmann, *Int. J.Quantum Chem.,* **2015**, DOI: 10.1002/qua.24882; G. Jindal, H. K. Kisan, R. B. Sunoj. *ACS Catal.* **2015**, *5*, 480–503.

[25] a) N. T. Anh, O. Eisenstein, *Nouv. J. Chim.* **1977**, *1*, 61-70,, b) S. Feldgus, C. R. Landis, *J. Am. Chem. Soc.* **2000**, *122*, 12714- 12727, c) M. Yamakawa, I. Yamada, R. Noyori, Angew. Chem. Int. Ed. **2001**, *40*, 2818-2821, d) S. Bahmanyar, K. N. Houk, *J. Am. Chem. Soc.* **2001**, *123*, 12911- 12912.

[26] E. H. Krenske, K. N. Houk, *Acc. Chem. Res.*, **2013**, *46,* 979–989.

[27] K. H. Hopmann, L. Frediani, A. Bayer, *Organometallics* **2014**, *33*, 2790-2797.

[28] T. Wang, L.-G. Zhuo, Z. Li, F. Chen, Z. Ding, Y. He, Q.-H. Fan, J. Xiang, Z.-X. Yu, A. S. C. Chan, *J. Am. Chem. Soc.* **2011**, *133*, 9878-9891.

[29] K. H. Hopmann, A. Bayer, *Organometallics* **2011**, *30*, 2483-2497.

[30] M. Yamakawa, I. Yamada, R. Noyori, *Angew. Chem. Int. Ed.* **2001**, *40*, 2818-2821.

[31] S. Qu, H. Dai, Y. Dang, C. Song, Z.-X. Wang, H. Guan, *ACS Catal.* **2014**, *4*, 4377-4388.

[32] X. Yang, M. B. Hall, *J. Am. Chem. Soc.* **2009**, *131*, 10901-10908.

[33] A. von der Höh, A. Berkessel, A. *ChemCatChem* **2011**, *3*, 861-867.

[34] S. Moulin, H. Dentel, A. Pagnoux-Ozherelyeva, S. Gaillard, A. Poater, L. Cavaloo, J.-F. Lohier, J.-L. Renaud, *Chem. Eur. J.* **2013**, *19*, 17881-17890.

[35] X. Lu, R. Cheng, N. Turner, Q. Liu, M. Zhang, X. Sun, *J. Org. Chem.* **2014**, *79*, 9355- 9364.

[36] H. Zhang, D. Chen, Y. Zhang, G. Zhang, J. Liu, *Dalton Trans.* **2010**, *39*, 1972-1978.

[37] Jindal, G.; Sunoj, R. B. *J. Org. Chem.* **2014**, *76*, 7600−7606.

[38] H. Li, J. Jiang, G. Lu, F. Huang, Z.-X. Wang, *Organometallics*, **2011**, *30*, 3131- 3141.

[39] M. Martin, E. Sola, S. Tejero, J.L. Andres, L.A. Oro, *Chem. Eur. J.* **2006**, *12*, 4043-4056.

[40] A. Comas-Vives, G. Ujaque, A. Lledós *Organometallics* **2008**, *27*, 4854.

[41] T. Nagano, A. Iimuro, R. Schwenk, T. Ohshima, Y. Kita, A. Togni, K. Mashima, *Chem. Eur. J.* **2012**, *18*, 11578-11592.

[42] W. Tang, S. Johnston, J.A. Iggo, N.G. Berry, M. Phelan, L. Lian, J. Bacsa, J. Xiao, *Angew. Chem. Int. Ed.* **2013**, *52*, 1668-1672.

[43] G. E. Dobereiner, A. Nova, N. D. Schley, N. Hazari, S. J. Miller, O. Eisenstein, R. H. Crabtree, *J. Am. Chem. Soc.* **2011**, *133*, 7547-7562.

[44] R. Noyori, S. Hashiguchi, *Acc. Chem. Res.* **1997**, *30*, 97-102.

[45] K.-J. Haack, S. Hashiguchi, A. Fujii, T. Ikariya, R. Noyori, *Angew. Chem., Int. Ed. Engl.* **1997**, *36*, 285-288.

[46] S. Zhou, *Development of new homogeneous (enantioselective) hydrogenation catalysts based on bio-relevant metals*, Dissertation, University Rostock, **2011**.

[47] K. H. Hopmann, F. Himo, *Chem. Eur. J.* **2006**, *12*, 6898–6909.

[48] K. H. Hopmann, *Inorg. Chem.*, **2014**, *53*, 2760-2762.

[49] Tang, W.; Johnston, S.; Iggo, J.A.; Berry, N.G.; Phelan, M.; Lian, L.; Bacsa, J.; Xiao, J., *Angew. Chem. Int. Ed.* **2013**, *52*, 1668-1672.

[50] (a) A. D. Becke, *Phys. Rev. A* **1988**, *38*, 3098-3100, (b) C. Lee, W. Yang, R. G. Parr, Phys. Rev. B **1988**, *37*, 785-789.

[51] Gaussian 09, Revision D.01, M. J. Frisch, G. W. Trucks, H. B. Schlegel, G. E. Scuseria, M. A. Robb, J. R. Cheeseman, G. Scalmani, V. Barone, B. Mennucci, G. A. Petersson, H. Nakatsuji, M. Caricato, X. Li, H. P. Hratchian, A. F. Izmaylov, J. Bloino, G. Zheng, J. L. Sonnenberg, M. Hada, M. Ehara, K. Toyota, R. Fukuda, J. Hasegawa, M. Ishida, T. Nakajima, Y. Honda, O. Kitao, H. Nakai, T. Vreven, J. A. Montgomery, Jr., J. E. Peralta, F. Ogliaro, M. Bearpark, J. J. Heyd, E. Brothers, K. N. Kudin, V. N. Staroverov, T. Keith, R. Kobayashi, J. Normand, K. Raghavachari, A. Rendell, J. C. Burant, S. S. Iyengar, J. Tomasi, M. Cossi, N. Rega, J. M. Millam, M. Klene, J. E. Knox, J. B. Cross, V. Bakken, C. Adamo, J. Jaramillo, R. Gomperts, R. E. Stratmann, O. Yazyev, A. J. Austin, R. Cammi, C. Pomelli, J. W. Ochterski, R. L. Martin, K. Morokuma, V. G. Zakrzewski, G. A. Voth, P. Salvador, J. J. Dannenberg, S. Dapprich, A. D. Daniels, O. Farkas, J. B. Foresman, J. V. Ortiz, J. Cioslowski, and D. J. Fox, Gaussian, Inc., Wallingford CT, 2013.

[52] (a) J. Tomasi, B. Mennucci, R. Cammi, R. *Chem. Rev.* **2005**, *105*, 2999-3093, (b) J. Tomasi, B. Mennucci, E. Cancès E. *J. Mol. Struct. (Theochem)* **1999**, *464*, 211-216, (c) E. Cancès, B. Mennucci, J. Tomasi, *J. Chem. Phys.* **1997**, *107*, 3032-3041.

[53] S. Grimme *J. Comput. Chem.* **2006**, *27*, 1787-1799.

[54] S. Grimme, J. Antony, S. Ehrlich, H. Krieg, *J. Chem. Phys*. **2010**, *132*, 154104.